OKU Fen Bilimleri Enstitüsü Dergisi
7(3): 1186-1201, 2024

OKU Journal of The Institute of Science and Technology, 7(3): 1186-1201, 2024

Osmaniye Korkut Ata Üniversitesi
Fen Bilimleri Enstitüsü
Dergisi

Osmaniye Korkut Ata University
Journal of The Institute of Science
and Technology

2009 A (H1N1) ve COVID-19 Pandemilerinde Nüfus Yoğunluğunun ve Temas Oranının Rolü

Ayşe PEKER DOBIE[1], Semra AHMETOLAN[2], Ayşe Hümeyra BİLGE[3], Ali DEMİRCİ[4*], Burak Erkan KAYA[5]

[1,2,4] İstanbul Teknik Üniversitesi, Fen- Edebiyat Fakültesi, Matematik Bölümü, İstanbul
[3,5] Kadir Has Üniversitesi, Mühendislik ve Doğa Bilimleri Fakültesi, Endüstri Mühendisliği Bölümü, İstanbul

[1]https://orcid.org/0000-0002-5228-7694
[2]https://orcid.org/0000-0003-1003-7918
[3]https://orcid.org/0000-0002-6043-0833
[4]https://orcid.org/0000-0001-9780-0132
[5]https://orcid.org/0000-0002-9110-0765
*Sorumlu yazar: demircial@itu.edu.tr

Araştırma Makalesi

Makale Tarihçesi:
Geliş tarihi: 12.10.2023
Kabul tarihi:24.01.2024
Online Yayınlanma: 25.06.2024

Anahtar Kelimeler:
A(H1N1)
Covid-19
Epidemi parametreleri
SIR modeli
Temel üreme sayısı
Temas oranı

ÖZ

Sağlıklı-Virus bulaşmış-Bulaşıcılığı olmayan (SIR) salgın modelinin başlıca özellikleri, temel üreme sayısı olarak bilinen R_0 parametresi tarafından belirlenir. Bu çalışmada, çeşitli Avrupa ülkeleri ve İstanbul'daki 2009 A(H1N1) pandemisi ile Almanya'nın federal eyaletlerindeki Covid-19 pandemisi olmak üzere iki farklı salgın için, R_0'ın temas oranlarına olan bağımlılığı araştırılmıştır. 2009 A(H1N1) pandemisine ait veriler, Hollanda da dahil olmak üzere yedi Avrupa ülkesi ve İstanbul için ele alınmış olup, bu ülkeler için temel üreme sayısının nüfus yoğunluğuna orantılı olduğu gösterilmiştir. Yüksek nüfus yoğunluklarına sahip olmaları nedeniyle Hollanda ve İstanbul'a ait R_0 değerlerinin, literatürde kabul edilen aralıkların oldukça dışında kaldığı gözlemlenmiştir. Covid-19 pandemisi için 2020 yılının Şubat ve Haziran ayları arasındaki döneme ait Almanya federal eyaletlerinin verileri kullanılarak, toplumdaki heterojenliklerin nüfus yoğunluğunun etkilerini domine ettiği gösterilmiştir. Bu durum, sokağa çıkma yasağı ve seyahat kısıtlamaları gibi uygulamaların ev içi dinamiklerinin rolünü arttırması olasılığı ile açıklanmıştır.

The Role of Population Density and Contact Rates for 2009 A (H1N1) and Covid-19 Pandemics

Research Article

Article History:
Received: 12.10.2023
Accepted: 24.01.2024
Published online: 25.06.2024

Keywords:
A(H1N1)
Covid-19
Epidemic parameters
SIR model
Basic reproduction number
Contact rate

ABSTRACT

Essential properties of the standard Susceptible-Infected-Removed (SIR) model are characterized in terms of the parameter, R_0, known as the basic reproduction number. In the present work, we investigate the dependency of R_0 on contact rates in two distinct cases, the 2009 A(H1N1) pandemic for European countries and Istanbul, and the Covid-19 pandemic for the federal states of Germany. For the data from the 2009 A(H1N1) pandemic, encompassing seven European countries (including the Netherlands) and Istanbul, Turkey, we show that the basic reproduction number is proportional to the population density. We observe in particular that for the Netherlands and for Istanbul, high population densities may give rise to parameters that lie well outside the accepted ranges in the literature. Using the data covering the period between February and June 2020, during the Covid-19 pandemic in the federal states of Germany, we observe that inhomogeneities in a population dominate the effects of population density, possibly due to the fact that curfew and travel restriction practices in force during that period enhance the role of household dynamics.

To Cite: Dobie AP., Ahmetolan S., Bilge AH., Demirci A., Kaya BE. 2009 A (H1N1) ve COVID-19 Pandemilerinde Nüfus Yoğunluğunun ve Temas Oranının Rolü. Osmaniye Korkut Ata Üniversitesi Fen Bilimleri Enstitüsü Dergisi 2024; 7(3): 1186-1201.

1. Introduction

The 2009 A(H1N1) swine flu and the ongoing Covid-19, while being devastating outbreaks, provided valuable epidemiological data, including fatality rates, hospitalization records, and PCR test results, particularly relevant to the current Covid-19 pandemic. All these records reflect the number of cases with some proportionality constant, which can vary depending on the location and may also change over time. For instance, the number of fatalities related to a particular disease is undoubtedly influenced by the quality of the healthcare system. In addition, the strength of contacts in a society, denoted as "contact rate", influences the number of cases.

While population density is known as one of the most important factors causing the spread of the disease (Chen and Li, 2020), research shows that due to socio-economic and cultural factors, more deaths are reported in sparsely populated areas than in densely populated areas, and this is strongly related to the contact rate. (Chen and Li, 2020; Hamidi et al., 2020). The crucial role of such factors is supported by studies that provide significant insights into the impact of such differences and of the age structure on the spread of COVID-19 cases. (Del Fava et. Al., 2020, Prem et. al., 2021). In addition to the primary influence of population density on contact rates, inhomogeneities in a society may lead to variations in the age structures and contact patterns and hence affect that rate.

In cases where social distancing measures are applied, demographic structures gain importance, and inhomogeneities in the population may lead to different contact rates within the same society. Thus, despite social distancing measures, co-residence of individuals from the same or different generations still have a noteworthy influence on the spread of the disease. (Esteve et. al., 2020). For example, individuals who are more susceptible to the disease, such as elderly people living in crowded multi-generational households for socio-economic and cultural reasons may lead to an increase in the spread of the disease. (Mogi and Spijker, 2022). Reducing contact rate via restrictions slows down the death rates and accelerates the recovery process. even if the population density is very high, (Ibrahim et. al., 2020). Thus, in cases where social distancing restrictions are applied in a homogeneous society, one would expect a decrease in the death rate proportional to the population density. However, the data of death rates for Covid-19 in the federal states of Germany displays a different pattern.

In the present work we discuss the role of the contact rate on the number of cases and fatalities, based on data of 2009 A(H1N1) swine flu and the Covid-19 pandemics. Data under consideration for 2009 A(H1N1) pandemic is the number of fatalities in Istanbul, Turkey, in seven European countries. Among these, the Netherlands and Istanbul, Turkey, are regions with considerably higher population densities. For these two cases, the parameters of the models describing the spread of the disease lie well outside the ranges reported in the literature, indicating the crucial role of the population density. Data for Covid-

19 pandemic in federal states of Germany is used to display the relation of the social/ethnic structures of the federal states on the number of Covid-19 cases., showing that although the population density is a main ingredient of the contact rate, inhomogeneities in the society may also affect the contact rate, hence the number of fatalities.

Numerous studies have focused on the 2009 A(H1N1) pandemic, examining its spread and characteristics. Some of these works were conducted at a country-specific level (Ergonul et. al., 2014; WHO, 2010; Tuite et. al., 2010), providing insights into the epidemic's progression within individual nations. Some works were based on the comparison of the characteristics of epidemic on transnational basis (WHO, 2009; Boëlle, 2011; Simonsen et. al., 2013; Bilge et. al., 2015; Samanlioglu and Bilge, 2016). In these works, epidemiological parameters such as basic reproduction number, infectious period and incubation period are estimated.

The basic reproduction number, the most crucial one among the epidemiological parameters, can be determined by the knowledge of the total proportion of individuals affected by the disease. This proportion can be measured by total fatalities, or total hospital referrals, or total positive cases. However, fatalities have a dependency on the healthcare systems, as analyzed for European countries during the 2009 A(H1N1) pandemic (Bilge and Samanlioglu, 2018). Hospital referrals are influenced by the severity of the disease. In addition, the coverage of tests is heavily dependent on the availability of tests within a society and the testing policies in place. An alternative method for determining the basic reproduction number is fitting models to the time-evolution of the normalized fatality or hospitalization data and choosing parameters of the models that fit with the smallest error.

The Basic Reproduction number, $\boldsymbol{R_0}$ represents the product of the transmission rate (parameter $\boldsymbol{\beta}$ in equation 1) and the mean duration of the infectious period (reciprocal of parameter $\boldsymbol{\gamma}$ in equation 1). The transmission rate $\boldsymbol{\beta}$ is itself the product of the virulence of the virus and of the contact rate. Determining accurate contact rates within a society is a complex process (Prem et. al., 2017). At a first approximation, one may assume that the contact rate is proportional to the population density, but at a finer scale, inhomogeneities in the population may dominate variations in the contact rates.

In our current study, we build upon the findings of our previous work analyzing the 2009 A(H1N1) data for Europe and for Istanbul. We utilize these results to demonstrate that the basic reproduction number fits to linear regression in terms of the population density, as expected, providing further proof of the validity of the standard SIR model. These results also indicate that the parameter $\boldsymbol{R_0}$ can be much higher than the values reported in the literature in cases of extreme population densities.

The second case that we analyze is the variation of total Covid-19 cases during the first wave of the pandemic, in various federal states of Germany. In this case, we observed that the burden of the epidemic is relatively insensitive to the population density, possibly due to strict restrictions that were effective particularly during the first wave. On the other hand, the variation of the ratio of total cases is correlated with the ratio of foreign population, as an indication of the household structure that is more relevant at times of curfew.

In comparison to the 2009 A(H1N1) pandemic, the Covid-19 pandemic has presented an extensive amount of epidemic data due to its widespread and global impact. However, it is worth noting that, apart from the initial stages, strict measures of various kinds have been implemented in almost all countries to control and mitigate the spread of Covid-19. These measures have significantly influenced the dynamics of the pandemic. Given this context, the 2009 A(H1N1) data, despite its relative simplicity, remains a valuable resource for modeling the spread of an epidemic in an uncontrolled population. The data captures the dynamics of an epidemic in a population without the strict measures and interventions that have been implemented during the Covid-19 pandemic. This allows researchers to gain insights into the natural course of an epidemic in a population without the influence of extensive control measures, providing a useful point of reference for understanding and modeling the spread of infectious diseases.

The article is organized as follows. In Section 2, we outline the mathematical models used for the standard SIR (Susceptible-Infected-Removed) model. Section 3 is devoted to the discussion of the role of population density on the contact rates, hence on $\boldsymbol{R_0}$, presenting the results obtained from analyzing two specific pandemics, specifically for the Netherlands in Section 3.1 and for Istanbul, Turkey in Section 3.2. In Section 4, we shift our focus to the 2020 Covid-19 pandemic in Germany, with the aim of investigating the role of heterogeneities in a population. Finally, in Section 5, we present our concluding remarks, summarizing the key findings from our study and discussing their implications.

2. Material and Methods

Compartment models in epidemiology are fundamental for the dynamics of the spread of a disease within a population (Kermack and McKendrick, 1927; Hethcote and Tudor, 1980). In these models the population is divided into compartments. The Susceptible-Infectious-Removed (SIR) and Susceptible-Exposed-Infectious-Removed (SEIR) models are prototypes of such models, commonly used to describe the spread of epidemics caused by a particular strain of infectious agent that primarily spreads through direct contact. In these models, individuals are initially categorized as susceptible to the disease. Upon contact with an infected individual, susceptible individuals transition to the infectious state. If the infecting agent has an incubation period, individuals who are infected but not yet infectious are placed in the "Exposed" compartment. During this incubation period, individuals cannot transmit the infection to others. Once the incubation period is over, individuals move to the "Infectious" compartment, where they can transmit the infection to susceptible individuals. Individuals in the "Infectious" compartment either recover from the infection or experience fatal outcomes within the infectious period. In either case, they are considered "removed" from the population, as they gain permanent immunity or are no longer able to transmit the infection.

The SIR epidemic model without vital dynamics is defined by

$$\boldsymbol{SIR}:\ \frac{d\boldsymbol{S}}{d\boldsymbol{t}} = -\boldsymbol{\beta S I}, \qquad \frac{d\boldsymbol{I}}{d\boldsymbol{t}} = \boldsymbol{\beta S I} - \boldsymbol{\gamma I},\ \ \frac{d\boldsymbol{R}}{d\boldsymbol{t}} = \boldsymbol{\gamma I}$$

(1)

where $\boldsymbol{\beta}, \boldsymbol{T} = \mathbf{1}/\boldsymbol{\gamma}$ refer to the disease transmission rate and to the mean duration of infection period respectively. The ratio, $\boldsymbol{\beta}/\boldsymbol{\gamma}$, corresponds to the basic reproduction number $\boldsymbol{R_0}$. As the sum of the righthand sides of these equations is zero, with appropriate normalization, one can choose $\boldsymbol{S} + \boldsymbol{I} + \boldsymbol{R} =$1. The SEIR model involves in addition an incubation period. In previous work (Bilge et. al., 2015), we have shown that for relatively low $\boldsymbol{R_0}$ values, diseases obeying the SEIR model can be well approximated by the SIR model, and in the following, we will restrict our work to the SIR model.

We also note that, as presented in (Bilge et. al., 2015), the parameter $\boldsymbol{R_0}$ can be determined from the knowledge of a single quantity, the final values of removed individuals at the end of epidemic, that we denote as $\boldsymbol{R_f}$. However, due to the lack of information on the exact values of fatality and hospitalization rates, in practice, we cannot use this information to evaluate $\boldsymbol{R_0}$. In fact, in the case of the 2009 A(H1N1) data, we have shown that fatality rates are in general correlated with health indices published by international organizations (Samanlioglu and Bilge, 2016), indicating the need to use more sophisticated methods. When working with data from different countries, we normalize epidemic data, and we estimate parameters by fitting models to the time evolution of the data. This approach, although more time-consuming, is well-suited for studying data from countries with diverse healthcare practices.

The results presented in Section 3, on the dependency of $\boldsymbol{R_0}$ on the population density uses the values of $\boldsymbol{R_0}$ evaluated from the time evolution of cumulative fatalities in different countries. On the other hand, in Section 4, as we study variations in $\boldsymbol{R_0}$ in various districts of the same country, with equally well health practices, we use the total number of cases in each district, to estimate $\boldsymbol{R_0}$ from its correspondence with $\boldsymbol{R_f}$.

3. Results and Discussion

3.1. The 2009 A(H1N1) Pandemic in Europe

In a previous work (Samanlioglu and Bilge, 2016), an analysis of weekly fatality data from 13 European countries was performed using reports from the European Centre for Disease Prevention and Control (ECDC) (ECDC, 2010). Data from the Czech Republic, France, Germany, the Netherlands, Norway, Romania, and Sweden were used for this analysis, and results reported in (Samanlioglu and Bilge, 2016), are summarized in Table 1. The method mentioned above was initially applied to analyze the 2009 A(H1N1) pandemic, and later, extended to study the Covid-19 pandemic (Ahmetolan et. al., 2020).

Table 1. Population density and the Basic Reproduction Number R_0 for 7 European countries.

Country	**Population Density**	$\boldsymbol{R_0}$
Czech Republic	132.72	1.5963
France	100.01	2.0118
Germany	229.68	2.7454
The Netherlands	396.99	4.0000
Norway	12.45	1.5782
Romania	90.18	1.4806
Sweden	20.57	1.5782

The estimated values reported in (Samanlioglu and Bilge, 2016), for 2009 A(H1N1) pandemic generally fell within the ranges reported in the existing literature. However, the values obtained for the Netherlands deviated from these ranges, and we refrained from reporting our findings for the Netherlands in that publication. Similarly, the method was also applied to analyze daily hospitalization and fatality reports collected from major hospitals in Istanbul during the same pandemic, and the estimated parameter values for this case were also found to be outside the ranges reported in the literature. These results seemed to suggest unique characteristics of the epidemics in the Netherlands and Istanbul, which may warrant further investigation of the role of population density in understanding the dynamics and impact of the respective pandemics in regions with different population dynamics. In Sections 3.1 and 3.2, we present the results of our analysis for the estimation of epidemic parameters for 2009 A(H1N1) pandemic in the Netherlands and in Istanbul, Turkey, respectively.

In Table 1 and Figure 1, we present the dependency of $\boldsymbol{R_0}$ on the population density, based on the estimates given in (Samanlioglu and Bilge, 2016).

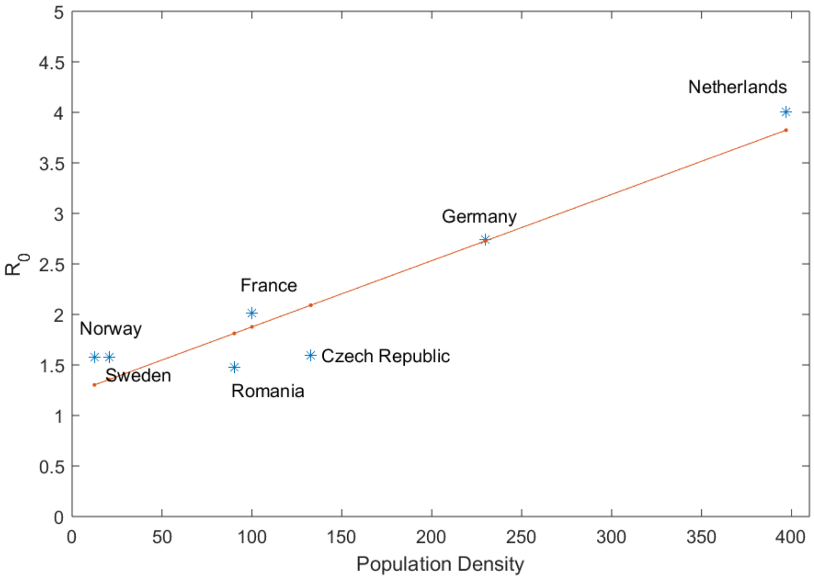

Figure 1. R_0 versus populaton density for European countries. Parameters are computed using the time evolution of normalized data.

A plot of R_0, as determined from the time evolution of the weekly fatality data is shown in Figure 1 above, together with a linear regression line. We describe below the analysis of the data for the Netherlands, in greater detail.

3.1.1. Determination of Epidemic Parameters for the Netherlands Data

In a previous study (Samanlioglu and Bilge, 2016), an examination of weekly fatality data for 13 European countries was performed using reports from the European Centre for Disease Prevention and Control (ECDC). The Netherlands was considered for the analysis of vaccination coverage etc, but its data was found to contain errors and was subsequently excluded from the time domain analysis in (Samanlioglu and Bilge, 2016). In this section, we will focus on analyzing the data specifically for the Netherlands. Firstly, we will correct any obvious errors present in the data. Subsequently, we will explore and assess various models to determine the best fit based on various error criteria. It is important to note that in all cases studied, the calculated value of R_0 for the Netherlands was found to be larger than the values reported in the existing literature. This discrepancy highlights the unique characteristics and dynamics of the epidemic in the Netherlands. For reference, the weekly fatality data for the Netherlands can be found in (Samanlioglu and Bilge, 2016).

Figure 2 illustrates the change in the total fatality numbers in weeks, based on the corrected data from the ECDC weekly reports for the Netherlands.

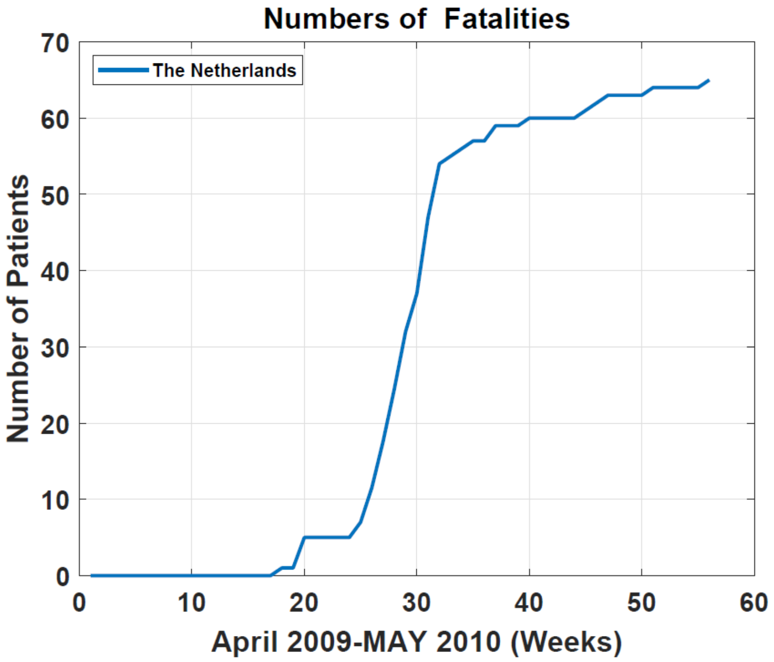

Figure 2. Cumulative number of fatalities for the 2009 A(H1N1) epidemic in the Netherlands, based on data Table A, corrected for obvious reporting errors in the data.

To further analyze the data, the normalized total fatality numbers for the Netherlands were fitted to the $R(t)$ curves obtained by numerical solutions of the SIR model with parameters over a reasonably wide range, and models within an "acceptable" error range were selected. For the Netherlands data, parameter ranges were chosen as, $1.5 \leq R_0 \leq 8$ in steps of 0.1 for the Basic Reproduction Number, $2 \leq T \leq 20$ in steps of 1 days for the mean duration of the infectious period, and $I(0) = 10^{-k}$ where $1 \leq k \leq 10$ in steps of 0.2 for the initial value for $I(t)$. With these parameter values, different simulations were compared. In order to select the best fitting model, two error criteria have been used: E_1, which covers the entire observation period, and E_2, which gives more weight on the initial phase of the epidemic. The time intervals taken into account for each error criterion are determined as $0-56$ weeks for E_1 and $0-29$ weeks for E_2, respectively. Error thresholds are set as the error levels of "acceptable" models and they are chosen as $E_1 < 0.1$ and $E_2 < 0.19$. The intervals corresponding to the "acceptable" error values are $2.9-4.2$ for $\boldsymbol{R_0}$, $3-5$ days for T and 10^{-7}-10^{-9} for $\boldsymbol{I_0}$. It is also observed that high $\boldsymbol{R_0}$ values correspond to low total error while low R_0 values correspond to high errors in the initial phases. Even though the infectious period interval for the Netherlands lies within reasonable bounds of influenza epidemics, the intervals observed for $\boldsymbol{R_0}$ the Netherlands cases are outside the expected ranges for flu type epidemics. As the values for the mean duration of the infectious period is within the ranges in the literature, we may conclude that discrepancy of the values reported in the literature for R_0 and the ones obtained in our work is not caused by computational errors, but it reflects the characteristics of the epidemic in that country.

3.1.2. Determination of Epidemic Parameters for the Istanbul Data

In this section, we focus on determining the parameters of the SIR model for the 2009 A(H1N1) epidemic in Istanbul, Turkey. A further support for the dependency of R_0 on the population density is provided by the analysis of the 2009 A(H1N1) data collected in Istanbul. Istanbul, the most densely populated city in Turkey, with a population of 12.92 millions and with a population density of 2431 persons/km^2, in 2009 (Source: Turkish Statistical Institute), serves as an important case study.

In the context of an extensive survey on the 2009 A(H1N1) epidemic (Ergonul et. al., 2014), information on (adult) patients referred to major hospitals in Istanbul, Turkey, were collected. The available data for this analysis consists of hospital records collected from six major state hospitals during the period of May 2009 to February 2010 (Ergonul et. al., 2014). To ensure consistency in the analysis, the first wave of the epidemic, which occurred between June 2009 and September 2009 and had no fatalities, is excluded from the dataset. Therefore, the analysis is based on a 200-day period spanning from September 1, 2009, to February 28, 2010. The data for the second wave of the epidemic consist of 869 cases of hospital referrals and the date of fatality of 46 patients. This dataset includes information such as the date of referral to the hospital, the date when symptoms started (as reported by the patient), the discharge date (which coincides with the referral date if the patient was not hospitalized), the date of transfer to the intensive care unit (if applicable), and the date of fatality. In Figure 3, we present the raw data for hospital referrals and cumulative fatalities.

Through the analysis of this data, we will obtain model parameters that once again fell outside the typical ranges reported in the literature. The consistent pattern of high $\mathbf{R_0}$ values observed in both the

Netherlands and Istanbul highlights the significant role of population density in understanding the dynamics of epidemic spread. The findings of Istanbul provide additional evidence for the influence of population density on disease transmission, emphasizing its importance in analyzing and interpreting epidemic patterns.

Our analysis starts with the following ranges: $1.5 \leq \boldsymbol{R_0} \leq 8$ (0.1 steps), $2 \leq \boldsymbol{T} \leq 20$ (1 steps) and $1 \leq k \leq 10$ (0.2 steps) where $\boldsymbol{I(0)} = 10^{-k}$ and we use the least squares error norm as the performance criteria, computed as follows. Assume that we want to obtain the error in modeling data represented by the column vector X, by a theoretical model represented by the column vector Y, both of length n. In matrix notation, the least squares error can be conveniently computed by $\sqrt{(X-Y)^t(X-Y)}$. Here we will be interested in the relative error, hence we define the error E as

E= $\sqrt{(X-Y)^t(X-Y)}$ / $\sqrt{X^tX}$

where the superscript t denotes the transpose.

To take into account extended hospitalization periods, we compute least squares errors for the beginning ($E_1: 0-80$ days) and for the intermediate ($E_2: 81-100$ days) periods. The error thresholds are chosen $E_1 < 0.04$ and $E_2 < 0.13$.

73 different simulations for the parameter intervals and the error bounds are also compared. The intervals corresponding to the minimum error values are 4.2-5.4 for $\boldsymbol{R_0}$, 13-15 for $\boldsymbol{T}$ and $10^{-7} - 10^{-8.8}$ for $\boldsymbol{I_0}$. It is also observed that high $\boldsymbol{R_0}$ values correspond to low total error while low $\boldsymbol{R_0}$ values correspond to high errors in the initial phases.

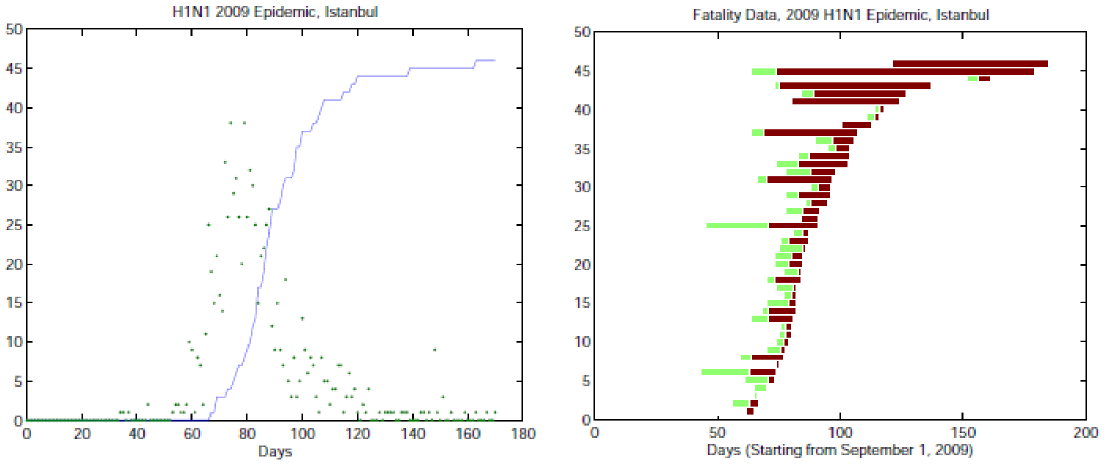

Figure 3. The daily number of referrals to hospitals and cumulative number of fatalities for the 2009 A(H1N1) epidemic in Istanbul, Turkey. The scatter in the number of daily referral to hospitals indicates that the hospitalization rate varies during the epidemic. The asymmetry of the incidence curve is still observable. The fatalities shown here are adjusted to at most 15 days after referral to the hospital (left panel). The duration of symptoms prior to hospitalization (light color) and the duration of hospitalization prior to death (dark color) for the fatalities during the epidemic in Istanbul are shown in the right panel.

To summarize our findings for the 2009 A(H1N1) for Istanbul, Turkey and for the Netherlands, the epidemic parameters $\boldsymbol{R_0}$ and $\boldsymbol{T}$ (mean duration of the epidemic) are found to be in the ranges $4.2-5.4$, $13-15$ days and $2.9-4.2$, $3-5$ days, respectively. The values for $\boldsymbol{R_0}$ which fall outside the usual influenza epidemic parameter values are interpreted by the high population density of both regions. The mean duration of the epidemic for the Netherlands is the same with the values in the literature for other European countires. Larger values of $\boldsymbol{T}$ for Istanbul may be tied to the failure of taking into account extended hospitalization periods.

3.2. The Covid-19 in Germany

In this section, the focus is on studying the Covid-19 data for Germany, from February to June 2020. This time frame captures the early stages and initial spread of the Covid-19 pandemic in Germany, and it can be considered as the first wave of the epidemic. The data consist of total cases for the federal states, and it can be interpreted as the final value of the removed individuals at the end of the first wave. As the same health care practices were effective over the whole country, we may assume that the proportionality constant between confirmed cases and total infections is the same for all states, therefore total number of cases represents the final value of removed individuals $\boldsymbol{R_f}$, in each state with the same proportionality constant. Furthermore, as the original virus was dominant during that period, variations in $\boldsymbol{R_0}$ arise from variations in the contact rate only. Thus, the scatter plot of the total number of cases versus the contact rate should follow the variation of $\boldsymbol{R_f}$ versus $\boldsymbol{R_0}$ after appropriate scalings.

Total population, foreign population, total cases, population densities and relevant ratios for the federal states are given below in Table 2.

In Figure 4 above, we present the scatter plot of the ratio of total cases with respect to population density. In this plot, we clearly see a cluster structure; the 3 city-states, Berlin, Hannover and Bremen, and the other states form 2 clusters, but unlike the 2009 A(H1N1) data for European countries, there is no obvious dependency on the population density.

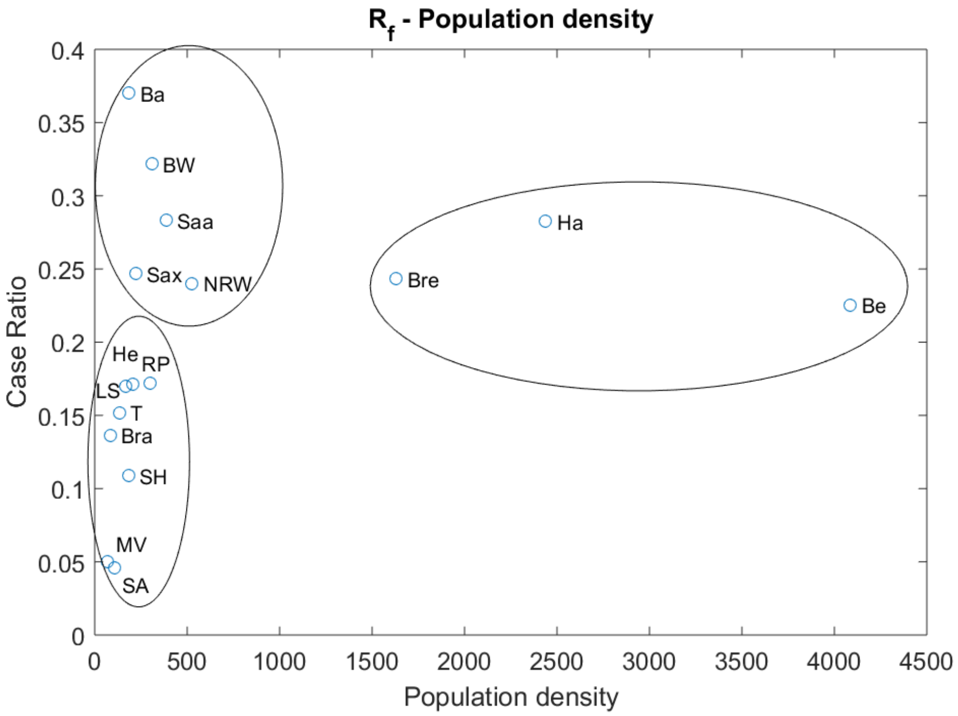

Figure 4. Percentage of cases versus population density.

On the other hand, the scatter plot of case ratios versus the ratio of foreign population, shown on Figure 5, displays a functional dependency. The 3 city-states still appear to form a separate cluster, and data of Bavaria seems to be an outlier.

We aim to quantify the relation between $\boldsymbol{R_0}$ and the population density and the density of the foreign population as observed in Figure 4 and Figure 5. Recall that $\boldsymbol{R_0}$ is known to be in the form $\boldsymbol{R_0 = \nu\, C\, T}$ where ν is the the virulence of the virus, $\boldsymbol{C}$ is the contact rate and $\boldsymbol{T}$ is the duration of the infectious period. Since **ν** and $\boldsymbol{T}$ are invariants of our data, the variation in $\boldsymbol{R_0}$ is directly proportional to $\boldsymbol{C}$.

We aim to obtain a bilinear model for the contact rate, hence for R_0, since it is a constant multiple of C, in the form,

$$R'_0 = C_0 + C_1 \text{(population density)} + C_2 \text{(ratio of foreign population)} \tag{2}$$

where C_0, C_1 and C_2 are constants to be determined and R'_0 denotes the least squares estimate of R_0. For this purpose we proceed as follows.

R_0 and the final proportion of removed individuals obey the formula $\boldsymbol{R_0 = -ln(1 - R_f)/R_f}$, as given by equation 2. In this formula, we replace $\boldsymbol{R_0}$ by $\boldsymbol{\nu\, C\, T}$ to obtain

$$\boldsymbol{\nu\, C\, T = -ln(1 - R_f)/R_f} \tag{3}$$

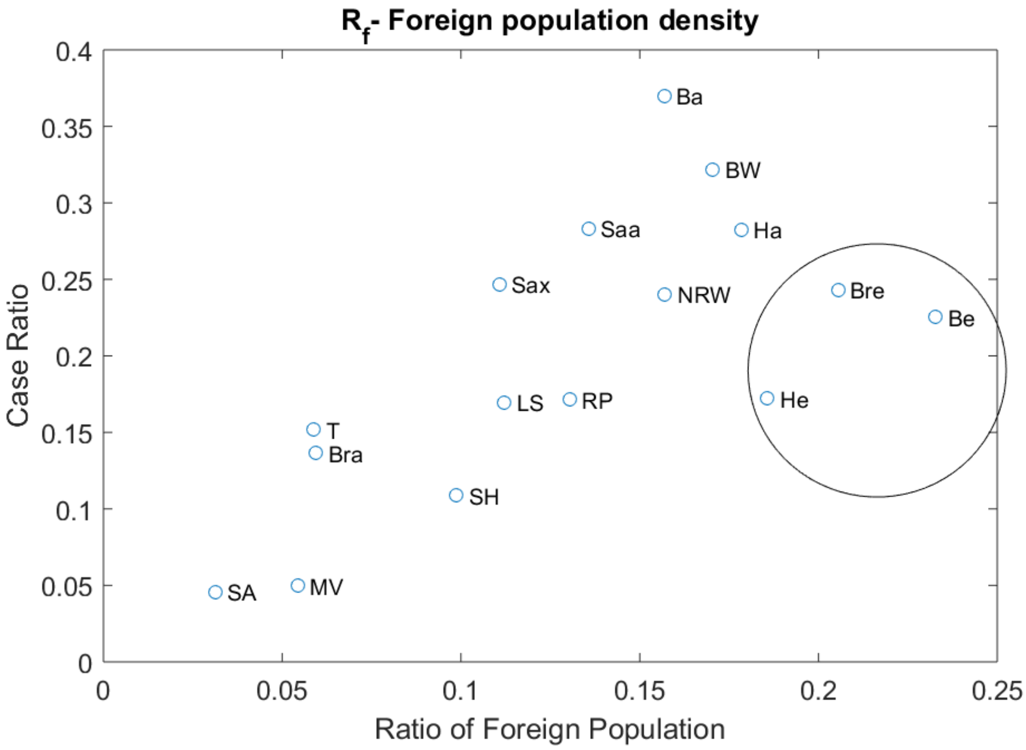

Figure 5. Percentage of cases versus the ratio of foreign population.

Table 2. Demographic information and Covid-19 case records for the federal states of Germany.

Province	**Population**	**Foreign**	**Ratio of Foreign Population**	**Total Cases**	**Percentage of Total Cases**	**Population Density**
Baden-Württemberg	11069533	1885925	0.1704	35620	0.3218	310
Bavaria	13076721	2051505	0.1569	48400	0.3701	185
Berlin	3644826	848400	0.2328	8220	0.2255	4,086
Brandenburg	2511917	149540	0.0595	3429	0.1365	85
Bremen	682986	140330	0.2055	1662	0.2433	1,630
Hamburg	1841179	328375	0.1784	5201	0.2825	2,439
Hesse	6265809	1163800	0.1857	10795	0.1723	297
Lower Saxony	7982448	895490	0.1122	13535	0.1696	168
Mecklenburg-Vorpommern	1609675	87410	0.0543	802	0.0498	69
North Rhine-Westphalia	17932651	2815800	0.1570	43066	0.2402	526
Rhineland-Palatinate	4084844	532230	0.1303	6996	0.1713	206
Saarland	990509	134350	0.1356	2806	0.2833	386
Saxony	2208321	244415	0.1107	5448	0.2467	221
Saxony-Anhalt	4077937	127670	0.0313	1871	0.0459	108
Schleswig-Holstein	2896712	286270	0.0988	3154	0.1089	183
Thuringia	2143145	126270	0.0589	3254	0.1518	133

Based on the assumption that $\boldsymbol{R_f}$ and $\boldsymbol{C}$ are proportional to case ratios and contact rates, respectively, we anticipate that they will obey the same functional relationship up to scalings, as described by equation 3. Consequently, we seek to establish a bilinear regression that relates C as defined above, where $\boldsymbol{R_f}$ is replaced by a constant multiple k of case ratios. To ensure consistency, the proportionality constant k needs to be selected in a manner that allows the percentage of total cases, multiplied by k, to fall within reasonable ranges. Additionally, the estimated values of $\boldsymbol{R_0}$ should be consistent with the values reported in the existing literature. Considering these factors, we have chosen the value of k to be 2.

Bilinear regression after excluding Bavaria and 3 cities (Berlin, Hannover and Bremen) discloses the following parameters:

$$C_0 = 0.9997, \qquad C_1 = 0.4785, \qquad C_2 = 1.3771.$$

The parameter C_2, which represents the effect of the ratio of the foreign population in a state, carries more weight in the bilinear regression analysis compared to the population density. This suggests that the presence of foreign population has a significant influence on the contact rates and, consequently, the spread of the epidemic.

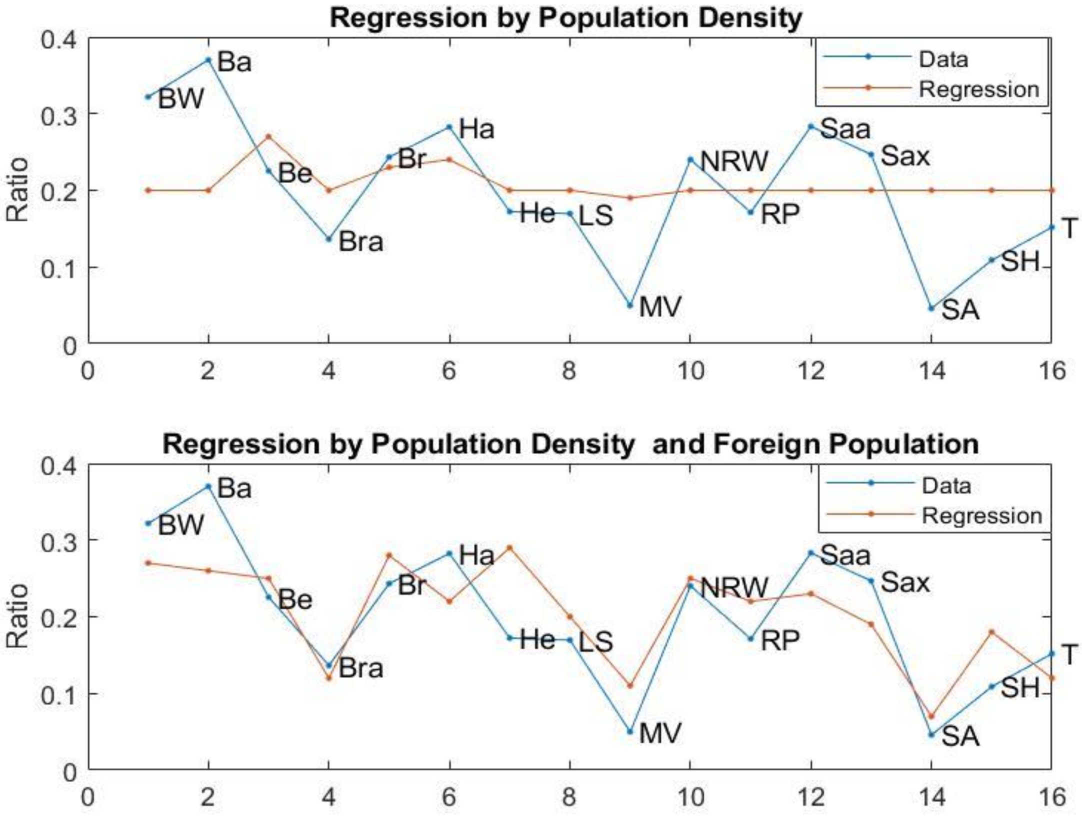

Figure 6. $\boldsymbol{R_f}$ versus $\boldsymbol{R_0}$. Theoretical (blue curve), regression (red data points).

In Figure 6, the solid line represents the curve of $\boldsymbol{R_f}$ versus $\boldsymbol{R_0}$, as computed from equation 2. The dots on this curve represent the pairs $(\boldsymbol{R_0}, \boldsymbol{R_f})$ obtained by replacing $\boldsymbol{R_f}$ with the total case ratio multiplied by a constant factor *k*, with *k* =2. The data points marked with (*) correspond to the pairs $(\boldsymbol{R_f}, \boldsymbol{R_0'})$, where $\boldsymbol{R_f}$ is as previously defined, and $\boldsymbol{R_0'}$ represents the estimated value for $\boldsymbol{R_0}$ obtained through the least squares regression. Additionally, the data points marked with (o) represent the estimates for Berlin, Bremen, Hamburg, and Bavaria, derived from the model. As expected, the model tends to overestimate $\boldsymbol{R_0}$ for Berlin, Bremen, and Hamburg, while underestimating it for Bavaria. These observations demonstrate the comparison between the computed values from the model and the estimated values obtained through regression. The deviations between the model estimates and the actual values highlight the variations in the epidemic dynamics and the influence of specific factors in different regions.

4. Conclusions

This article aims to illustrate the role of population density and the contact rates on the basic reproduction number. The effect of the population density is discussed via 2 cases, the data for the 2009 A(H1N1) epidemic in Istanbul and the Netherlands, while the effect of contact rates is analyzed for the Covid-19 data for the federal states of Germany.

To determine the epidemic parameters for the Istanbul data, we compare the normalized cumulative fatality data with the solutions of the SIR model. To obtain the best-fitting model, two different error criteria are employed. Parameter for best fitting models deviate from the typical values associated with influenza epidemics. Specifically, the minimum error values for the Istanbul data correspond to $4.2 - 5.4$ and $13 - 15$ for $\boldsymbol{R_0}$, and $\boldsymbol{T}$ respectively. These findings suggest that the 2009 A(H1N1) epidemic in Istanbul exhibits unique characteristics and differs from the usual patterns observed in influenza epidemics.

Similarly, we perform the same analysis to the Netherlands, with a similar population density. We compare the normalized cumulative fatality numbers from the weekly reports by the ECDC with the solutions obtained from the SIR model. Using the same error criteria employed for the Istanbul analysis, we determine the best-fitting model for the Netherlands. As a result, the minimum error values for the Netherlands data correspond to the parameter ranges of 2.9-4.2 for $\boldsymbol{R_0}$, 3-5 for $\boldsymbol{T}$, and 10^{-7}-10^{-9} for $\boldsymbol{I_0}$. These parameter ranges, similar to those found for Istanbul, deviate from the typical parameter values associated with influenza epidemics.

We note that variations in the contact rate cannot be solely attributed to population density. Cultural differences and societal factors can also play a significant role in shaping the strength of interactions within a community which may also affect the contact rate, hence the Basic Reproduction Number $\boldsymbol{R_0}$. To highlight this point, we extend our analysis to include the Covid-19 data for the federal states of Germany during the period from February to June 2020. In this analysis, as the quality of the health care is uniform overall Germany, we assume that the proportionality constant between confirmed cases and total infections remains the same across all federal states. Using the method of determining $\boldsymbol{R_0}$ from $\boldsymbol{R_f}$, we investigate the relationship between these parameters and various factors. Notably, we find that there is no evident dependency on population density, which contrasts with our observations from the 2009 A(H1N1) data for European countries. Instead, our analysis reveals that the ratio of the foreign population within a state holds more weight in the regression analysis compared to population density. This suggests that demographic factors, such as the presence of foreign inhabitants, exert a significant influence on the contact rate and consequently impact the determination of R_0.

Acknowledgment

We would like to thank Prof. Onder Ergonul for providing insight into the 2009 A(H1N1) data for Istanbul.

Conflict of Interest

The authors declare that the research was conducted in the absence of any commercial or financial relationships that could be construed as a potential conflict of interest.

Authors' Contributions

All authors contributed to the article and approved the submitted version.

References

Ahmetolan S., Bilge AH., Demirci A., Peker-Dobie A., Ergonul O. What can we estimate from fatality and infectious case data using the susceptible-infected-removed (SIR) model? A case study of covid-19 pandemic. Frontiers in Medicine 2020; 7: 556366.

Bilge AH., Samanlioglu F., Ergonul O. On the uniqueness of epidemic models fitting a normalized curve of removed individuals. Journal of Mathematical Biology 2015; 71(4): 767-794.

Bilge AH., Samanlioglu F. Determination of epidemic parameters from early phase fatality data: A case study of the 2009 A(H1N1) pandemic in Europe. International Journal of Biomathematics 2018; 11(2): 1850021.

Boëlle PY., Ansart S., Cori A., Valleron AJ. Transmission parameters of the A/H1N1 (2009) influenza virus pandemic: a review. Influenza and Other Respiratory Viruses 2011; 5(5): 306-316.

Chen K., Li Z. The spread rate of SARS-CoV-2 is strongly associated with population density. Journal of Travel Medicine 2020; 27(8): 1-2.

ECDC weekly influenza surveillance overview reports, Week 36 2009- Week 21 2010,

Del Fava E., Cimentada J., Perrotta D., Grow A., Rampazzo F., Gil-Clavel S., Zagheni E. The differential impact of physical distancing strategies on social contacts relevant for the spread of COVID-19: Evidence from a multi-country survey. MedRxiv 2020-05.

Ergönül Ö., Alan S., Ak Ö., Sargin F., Kantürk A., Gündüz A., et al. Predictors of fatality in pandemic influenza A (H1N1) virus infection among adults. BMC Infectious Diseases 2014; 14(1): 317.

Esteve A., Permanyer I., Boertien D., Vaupel JW. National age and coresidence patterns shape COVID-19 vulnerability. Proceedings of the National Academy of Sciences - PNAS 2020; 117(28): 16118-20.

Hamidi S., Sabouri S., Ewing R. Does density aggravate the COVID-19 Pandemic?: Early findings and lessons for planners. Journal of the American Planning Association 2020; 86(4): 495-509.

Hethcote HW., Tudor DW. Integral equation models for endemic infectious diseases. Journal of Mathematical Biology 1980; 9(1): 37-47.

Ibrahim AM., Mohammed Eid M., Mostafa NN., Mohamed Bishady NE., Elghalban SH. Modeling the effect of population density on controlling covid-19 initial spread with the use of MATLAB numerical methods and stringency index model. 2nd Novel Intelligent and Leading Emerging Sciences Conference (NILES) 2020, Paper no: 612-617.

Kermack WO., McKendrick AG. A contribution to the mathematical theory of epidemics. Proceedings of the Royal Society of London. Series A, Containing Papers of A Mathematical and Physical Character 1927; 115(772): 700-721.

Mogi R., Spijker J. The influence of social and economic ties to the spread of COVID-19 in Europe. Journal of Population Research 2022; 39(4): 495-511.

Prem K., Cook AR., Jit M. Projecting social contact matrices in 152 countries using contact surveys and demographic data. PLoS Computational Biology 2017; 13(9): e1005697.

Prem K., Zandvoort K., Klepac P., Eggo RM., Davies NG. Centre for the Mathematical Modelling of Infectious Diseases Covid-19 Working Group, Cook AR., Jit M. Projecting contact matrices in 177 geographical regions: An update and comparison with empirical data for the COVID-19 era. PLoS Computational Biology 2021; 17(7):e1009098.

Samanlioglu F., Bilge AH. An overview of the 2009 A(H1N1) pandemic in Europe: efficiency of the vaccination and healthcare strategies. Journal of Healthcare Engineering 2016; 2016: 1-13.

Simonsen L., Spreeuwenberg P., Lustig R., Taylor RJ., Fleming DM., Kroneman M, et al. Global mortality estimates for the 2009 influenza pandemic from the glamor project: a modeling study. PLoS Medicine 2013; 10(11): e1001558.

Tuite AR., Greer AL., Whelan M., Winter A., Lee B., Yan P, et al. Estimated epidemiologic parameters and morbidity associated with pandemic H1N1 influenza. Canadian Medical Association Journal (CMAJ) 2010; 182(2): 131-136.

WHO. Writing committee of the WHO consultation on clinical aspects of pandemic (H1N1) 2009 influenza. Clinical aspects of pandemic 2009 influenza A (H1N1) virus infection. The New England Journal of Medicine 2010; 362(18):1708-1719.

WHO. World Health Organization. Transmission dynamics and impact of pandemic influenza A (H1N1) 2009 virus, Weekly epidemiological record. November 2009; 84(46).